A Theoretical Study of the Reaction of GeH_2 with CO_2 and the Dissociation Paths of the Reaction Products

Suk Ping So* and Wai-Kee Li*

Department of Chemistry, The Chinese University of Hong Kong, Shatin, N.T., Hong Kong

Received: January 19, 2004; In Final Form: March 4, 2004

The energy profiles for the reaction between GeH_2 and CO_2 have been studied by the G2+ method, which is a modified Gaussian-2 model of theory. It is found that this reaction first yields loosely bound isomeric $H_2Ge\cdots OCO$ complexes **1** and **2**. These complexes can then undergo reactions leading to products H_2GeO + CO (reaction 1) or GeO + H_2CO (reaction 2). The G2+ results suggest that reaction 1 is more likely to take place. In addition, the dissociation of **1**/**2** should proceed via two intermediates, instead of the direct cleavage of a CO bond. The results reported here are also compared with the theoretical and experimental data of the analogous reaction between SiH_2 and CO_2.

1. Introduction

Silylene, SiH_2, has been found to be reactive toward many chemical species. Reactions such as Si−H bond insertion, C=C, C≡C, and C=O π-bond addition, and reactions with lone-pair electron donors[1−4] are rapid and efficient with rates close to collision rates. Meanwhile, methylene, CH_2, in its $^1A_1$ first excited state (note that the ground state of SiH_2 is $^1A_1$) is found[5] to react with CO_2, but with a relatively small second-order rate constant of about 3.3×10^{-11} cm^3 molecule^{-1} s^{-1} at room temperature. Experimental results suggest that the products of the reaction are H_2CO and CO and that α-lactone is a plausible intermediate.[5,6] Mechanistic calculations at the G2 level[7] reveal that the latter is indeed a stable intermediate in the reaction path of lowest energy for the production of H_2CO and CO. Recently, Becerra et al.[8] studied experimentally and theoretically the SiH_2 + CO_2 reaction to find out whether the affinity of SiH_2 for a carbonyl bond extends even to the highly stable CO_2 molecule. Their experimental kinetics data show that the reaction is extremely slow with a second order rate constant of about 1.7×10^{-15} cm^3 molecule^{-1} s^{-1} at 298 K, which is about 5 orders of magnitude slower than that for the SiH_2 + CO reaction, and has a positive activation energy of 3.9 kcal mol^{-1}. At the G2 level of theory, the mechanistic path, in which SiH_2 adds to a CO π-bond of CO_2 with the overall formation of H_2SiO and CO via the cyclic intermediate siloxiranone, is computed to be most favorable energetically with a barrier of 3.0 kcal mol^{-1} relative to the reactants. Besides, another much energetically less plausible path leading to the overall formation of SiO and CH_2O has also been predicted. However, this path involves a number of rearrangement activation barriers, the highest of which is 5.8 kcal mol^{-1} above the reaction threshold, i.e., SiH_2 + CO_2 (or 32.9 kcal mol^{-1} relative to the preceding species).

The reactions of germylene, GeH_2, the germanium analogue of SiH_2, with a few molecular species have been studied.[9] It is found that GeH_2 inserts readily into Si−H bonds (and probably Ge−H bonds), and adds rapidly (close to collision rates) to the π-bonds of alkenes, alkynes, and dienes. Nevertheless, the rates of these reactions are somewhat slower than those of the corresponding reactions involving SiH_2. To our knowledge, both experimental and theoretical studies of the reaction of GeH_2 with CO_2 have not been reported in the literature. Hence, as a continuation to our theoretical study on the GeH_2 + H_2O reaction,[10] it is desirable to study the potential energy surface for the reaction of GeH_2 with CO_2 to gain some insight into its mechanisms. The channels with initial electrophilic attack on an O atom or cycloaddition to a CO π-bond of CO_2 are considered.

2. Calculations

The structures of the various species studied were optimized by the energy gradient method at the restricted (for singlet states) and the unrestricted (for open-shell states) MP2(FU) level of theory (FU denotes full, meaning inclusion of both inner-shell and valence-shell electrons), using the GAUSSIAN 98 package of programs[11] implemented on our DEC 600 AU, and COMPAQ XP900 and XP1000 workstations. Various techniques were used to determine the transition state (TS) structures. Initial geometries were either estimated from the reactant and/or product structures, or located by partial geometry optimization with a structural parameter held at a series of fixed values. These initial geometries were then fully optimized, i.e., all geometrical parameters were allowed to vary, using the automated TS option of GAUSSIAN 98. If the initial symmetry of a species (equilibrium or TS structure) changed to a practically higher one on geometry optimization, its geometry was then reoptimized under the constraint of the latter symmetry. For example, geometry optimization under C_1 symmetry yielded a nearly C_s structure for the adduct GeH_2CO_2. Hence, it was reoptimized with the C_s symmetry constraint imposed.

The energies of the optimized structures were computed with the Gaussian-2 (G2) theory,[12] which is an improved version over the Gaussian-1 (G1) theory.[13,14] The conventional G2 method uses a series of frozen-core (FC) QCISDT, MP4SDTQ, and MP2 single-point energy calculations on the MP2(FU)/6-31G(d) structures with various basis sets to approximate a QCISDT-(FC)/6-311+G(3df,2p) calculation, incorporating a number of corrections to the total energy.[12] Zero-point vibrational energy corrections (ZPEs) are evaluated from the HF/6-31G(d) frequencies scaled by 0.8929. However, in the present work, the

* Address correspondence to these authors at the following: fax +852-2603-5057; e-mail sukpingso@cuhk.edu.hk or wkli@cuhk.edu.hk.

10.1021/jp0497209 CCC: $27.50
Published on Web 04/14/2004

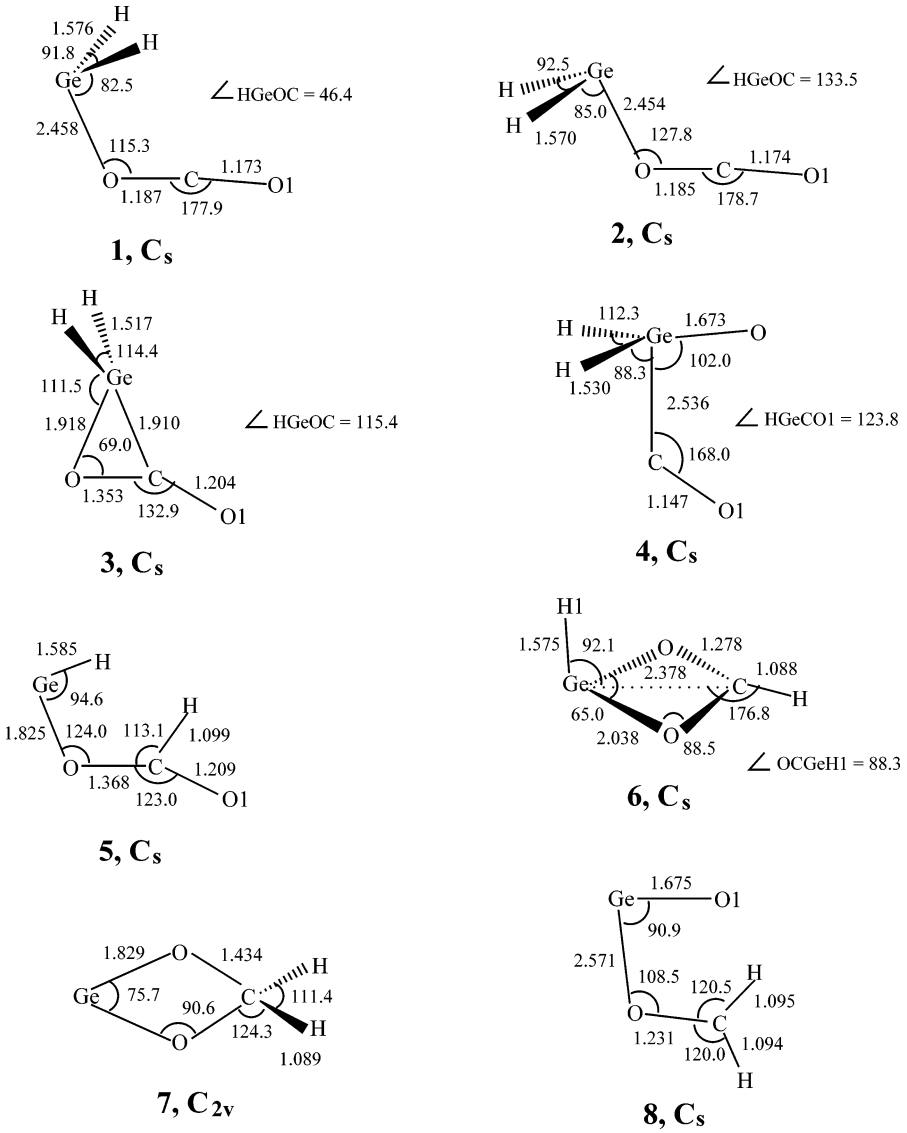

Figure 1. MP2(FU)/6-31+G(d,p) optimized equilibrium structures of the species studied. Bond lengths are in angstroms and angles in degrees.

modified G2 method, denoted as the G2+ method,[15] was used. In this method, MP2(FU)/6-31+G(d,p) geometries and vibrational frequencies (scaled by 0.9427; a factor suggested for frequencies calculated at this level[16]) are employed instead. In addition, the 6-311+G(m,p), instead of 6-311G(m,p), basis functions, where m = d or 2df, are used for the single-point energy calculations.

Vibrational frequencies were determined by the analytical evaluation of the second derivatives of energy to verify the nature (equilibrium or TS) of the stationary point structures optimized, to provide zero-point vibrational energy corrections, and to predict vibrational frequencies of the stable species for the sake of their identification by infrared spectroscopy.

The connection between a TS structure and its reactants and products was established, at the MP2(FU)/6-31+G(d,p) level of theory, by the intrinsic reaction coordinate (IRC) calculations based on the reaction path following the algorithm of Gonzalez and Schlegel[17,18] as coded in GAUSSIAN 98, or by optimization starting from a TS structure with one or two of its geometrical parameters distorted.

3. Results and Discussion

Figures 1 and 2 display the various stationary point structures studied together with their optimized geometrical parameters. Geometry optimization of structures **1** and **2** at the MP2(FU)/6-31G(d) level yields exceedingly long GeO bonds (2.492 and 2.494 Å, respectively), much longer than the experimentally determined GeO single bonds of, for example, $(H_3Ge)_2O$ (1.77 Å),[19] $((PhCH_2)_3Ge)_2O$ (1.73 Å),[20] and $(t\text{-}Bu_2(Me)PhO)_2Ge$ (1.81 Å).[21] Indeed, the GeO bonds are so long that it seems more appropriate to describe **1** and **2** as molecular complexes rather than normal molecules. Accordingly, the G2+ method[15] was used for this work in which the MP2(FU)/6-31G(d) geometries and HF/6-31G(d) frequencies employed in the G2 method are replaced by the MP2(FU)/6-31+G(d,p) geometries and frequencies. Besides, more elaborate basis sets are used in the single-point energy calculations (see above). The calculated structures have been shown to be either equilibrium structures (**1**, **2**, ..., **8**) or TS structures (**TS1/2**, **TS1/3**, **TS1/5**, **TS2/3**, **TS3/4**, **TS5/6**, **TS6/7**, **TS7/8**, **TS1d**, and **TS2d**) by their MP2(FU)/6-31+G(d,p) vibrational frequencies. In our notation, **TSx/y** denotes the TS structure for the isomerization reaction connecting reactants **x** and product **y**, while **TSxd** is the TS structure for the dissociation of species **x**. Table 1 lists the unscaled MP2(FU)/6-31+G(d,p) harmonic vibrational frequencies of the stable germanium-containing species studied together with experimental values available. Among the species calculated, the vibrational bands of only three of them, H_2GeO, GeH_2, and GeO,

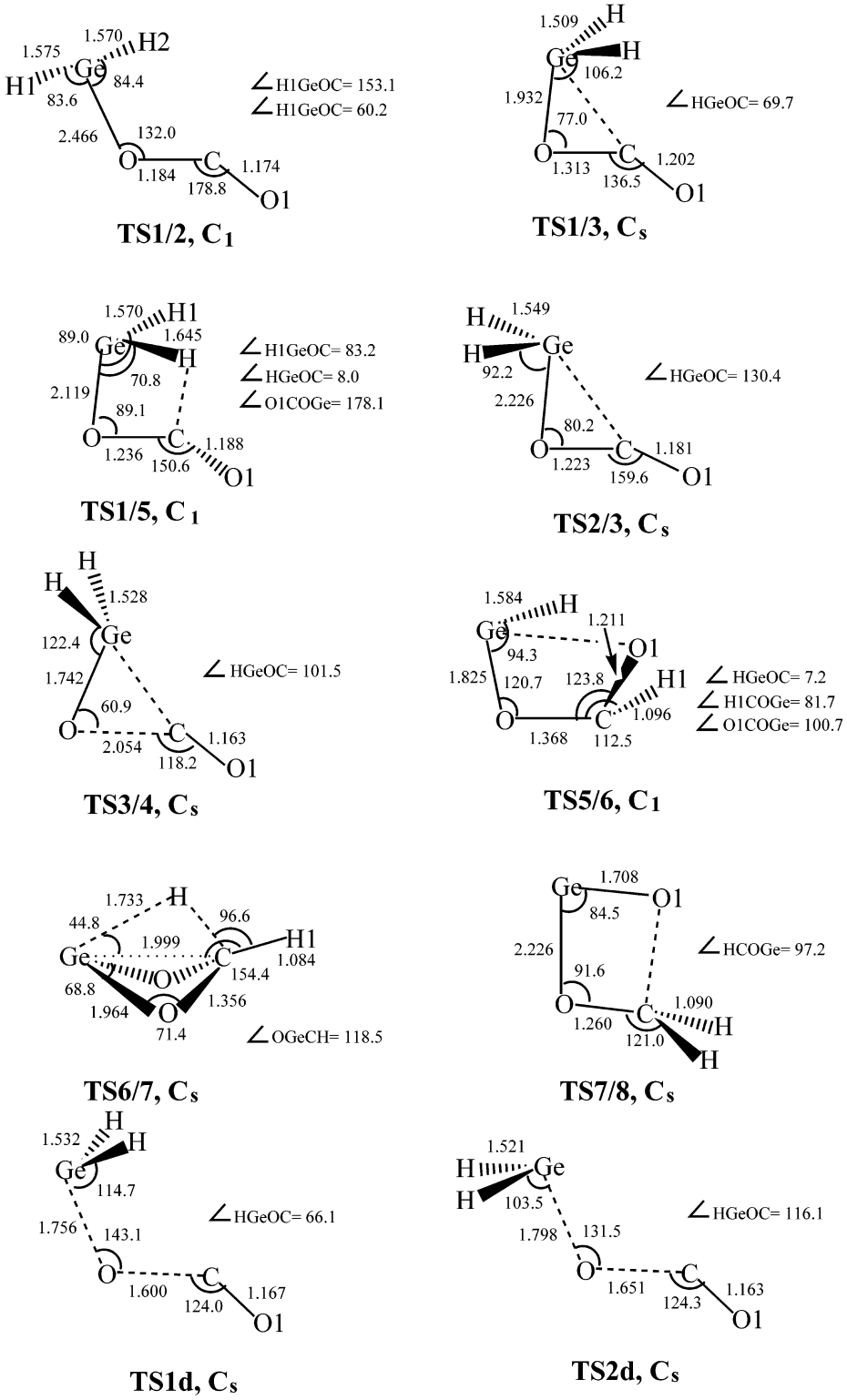

Figure 2. MP2(FU)/6-31+G(d,p) optimized transition state structures of the reactions studied. Bond lengths are in angstroms and angles in degrees.

have been observed and reported.[22,23] Since these observed bands are for the species in matrices, the agreement between the predicted and the observed frequencies may thus be considered as reasonable. Table 2 collects the G2+ total and relative energies of the species studied. The energy profiles for the reactions investigated are shown in Figure 3.

3.1. Reaction 1: 1/2 → H_2GeO + CO. An MP2(FU)/6-31+G(d,p) geometry optimization for the electrophilic attack of GeH_2 on an O atom of CO_2 yields the isomeric species **1** and **2**, while the cycloaddition of GeH_2 to a CO π-bond of CO_2 results in cyclic species **3**. Alternatively, **3** may also be generated from the cyclization of **1** or **2**. At the G2+ level, **1** and **2** are formed exothermically, but by 3.6 and 2.7 kcal mol^{-1} only, and thus they may readily dissociate back to the reactants. On the other hand, the above three channels for the formation of **3** are all endothermic since the latter is higher in energy than the two reactants by 5.1 kcal mol^{-1} (Table 2).

Species **1** and **2** are predicted to have very long GeO bonds (2.458 and 2.454 Å, respectively, Figure 1) even when the extended 6-31+G(d,p) basis set is used in the geometry

TABLE 1: MP2(FU)/6-31+G(d,p) Harmonic Vibrational Frequencies[a] of the Stable Ge-Containing Species Studied

species	vibrational frequencies (cm^{-1})
1	23.0, 54.2, 164.6, 498.9, 555.9, 639.9, 642.7, 984.4, 1319.2, 2072.3, 2091.3, 2416.1
2	35.0, 41.7, 149.8, 453.8, 505.5, 639.9, 642.4, 978.3, 1327.3, 2099.2, 2120.9, 2424.4
3	355.0, 357.3, 410.1, 561.8, 609.6, 633.2, 736.7, 896.3, 1080.2, 1868.1, 2342.7, 2357.5
4	54.5, 124.8, 181.2, 244.8, 470.8, 577.2, 701.0, 914.9, 952.6, 2143.6, 2272.1, 2286.0
5	99.7, 240.2, 339.8, 435.1, 818.5, 848.1, 1062.1, 1110.4, 1432.0, 1794.2, 2039.5, 3086.7
6	339.5, 346.1, 405.6, 604.3, 808.8, 842.8, 1058.6, 1342.6, 1402.2, 1602.1, 2089.3, 3231.4
7	299.9, 543.8, 620.0, 829.8, 952.3, 1059.8, 1158.0, 1188.1, 1386.9, 1587.9, 3136.0, 3210.3
8	118.7, 147.6, 183.1, 263.0, 321.9, 919.2, 1243.9, 1296.2, 1549.3, 1733.9, 3079.6, 3196.2
GeH_2	991.2 (920),[b] 2112.1 (1864), 2128.7 (1887)
H_2GeO	579.9, 602.2, 903.9 (803.8), 953.3 (961.9), 2303.0 (2079.6), 2307.1 (2076.6)
GeO	919.7 (970.4)

[a] Frequencies not yet scaled by the factor of 0.9427. [b] Observed matrix IR bands are in parentheses (GeH_2, ref 17; H_2GeO and GeO, ref 18).

TABLE 2: G2+ Total (hartree) and Relative (kcal mol^{-1}) Energies of the Species Studied

species	energy	rel energy
1	−2265.10648	−3.6
2	−2265.10502	−2.7
3	−2265.09257	5.1
4	−2265.07866	13.8
5	−2265.11655	−10.0
6	−2265.13577	−22.0
7	−2265.13901	−24.1
8	−2265.11048	−6.2
GeH_2	−2076.73979	
$GeH_2 + CO_2$	−2265.10067	0.0
H_2GeO	−2151.89912	
$H_2GeO + CO$	−2265.07641	15.2
GeO	−2150.76040	
$GeO + H_2CO$	−2265.09890	1.1
TS1/2	−2265.10528	−2.9
TS1/3	−2265.05492	28.7
TS1/5	−2265.08658	8.8
TS2/3	−2265.09044	6.4
TS3/4	−2265.06029	25.3
TS5/6	−2265.11431	−8.6
TS6/7	−2265.07225	17.8
TS7/8	−2265.08882	7.4
TS1d	−2265.02853	45.3
TS2d	−2265.01012	56.8

optimization. Besides, the geometrical parameters of the GeH_2 (GeH = 1.570−1.576 Å, ∠HGeH = 91.8−92.5°) and the CO_2 (CO = 1.173−1.185 Å, ∠OCO = 177.9−178.7°) subunits of these two structures are very close to the corresponding ones of the free GeH_2 (GeH = 1.570 Å, ∠HGeH = 91.8°) and CO_2 (CO = 1.180 Å) species. Thus **1** and **2** are loosely bound addition complexes of the type $H_2Ge\cdots OCO$, rather than normal molecules. Similarly, intermediates **4** and **8** (see below) may also be regarded as $H_2(O)Ge\cdots CO$ and $H_2CO\cdots GeO$ complexes, respectively (Figure 1). The silicon counterparts[8] of **1**, **2**, **4**, and **8** also have similar structural characteristics.

The TS structures for the formation of **1**, **2**, and **3** from GeH_2 and CO_2 have been searched at the MP2(FU)/6-31+G(d,p) level. But, unfortunately, the attempt was not successful. Thus, geometry optimizations were performed with their GeO bonds being kept fixed at various distances. It was found that the energies of **1** and **2** are still increasing when their GeO bonds are extended up to 5.50 Å. This suggests that the formation of **1** and **2** from GeH_2 and CO_2 occurs without a barrier. Additionally, the attempt to locate a TS linking **3** with reactants (GeH_2 and CO_2) also failed.

Complexes **1** and **2** may dissociate to the products (H_2GeO + CO) either by breaking their $H_2GeO\cdots CO$ bond (reaction pathway 1a: **1/2** → H_2GeO + CO) or via two consecutive endothermic rearrangements to the intermediates **3** and **4**, followed by a $Ge\cdots CO$ bond cleavage (reaction pathway 1b: **1/2** → **3** → **4** → H_2GeO + CO) as shown in Figure 3. Pathway 1a for **1** and **2** occurs via TS structures **TS1d** and **TS2d** (Figure 2) which are less stable than the reactants $GeH_2 + CO_2$ by 45.3 and 56.8 kcal mol^{-1} (i.e., with barriers of 48.9 and 59.5 kcal mol^{-1}) at the G2+ level, respectively. Thus, the dissociation pathway 1a will proceed faster for **1** than **2**, as far as only activation energy is concerned. In pathway 1b, **1** and **2** first cyclize to **3** via the TS structures **TS1/3** and **TS2/3**, respectively. Species **3** will then isomerize to **4** through the TS structure **TS3/4**. It should be noted that **TS1/3**, **TS2/3**, **TS3/4**, **3**, **4**, and products H_2GeO + CO are all less stable than $GeH_2 + CO_2$. The respective energies for these transition states relative to that of the reactants ($GeH_2 + CO_2$) are 32.3, 9.1, and 20.2 kcal mol^{-1}. The subsequent dissociation of **4** to H_2GeO and CO is barrierless and has an endothermicity of only 1.4 kcal mol^{-1}. The first step of pathway 1b is therefore much less favored energetically for **1** than **2**. As noted above, the exothermicity for the formation of **1** from GeH_2 and CO_2 is larger than that of **2** (Table 2). Nevertheless, the difference between them is only 0.9 kcal mol^{-1}. In addition, **1** can convert to **2** by an internal rotation of the GeH_2 group about the $Ge\cdots O$ bond via the TS structure **TS1/2**, which has a barrier of only 0.7 kcal mol^{-1}. Hence, **1**, even formed, should isomerize to **2** first before it dissociates. It should be noted that the rate-determining step for the dissociation of **2** to H_2GeO and CO in reaction pathway 1b is the rearrangement of **3** to **4**, which is associated with an activation energy of 20.2 kcal mol^{-1}, a value less than half of those for pathway 1a. Consequently, the dissociation of the $H_2Ge\cdots OCO$ complexes **1** and **2** to H_2GeO and CO results predominantly from the decomposition of **2** along the reaction pathway 1b.

It has been noted above that **1** converts to **2** via an internal rotation rather than an inversion at the Ge center. This may be accounted for as follows. Inversion at the Ge center requires Ge to acquire a near-trigonal planar local symmetry in which the Ge valence orbitals become sp^2-hybridized. It is well-known that hybridization of the valence s- and p-orbitals is more difficult energetically for the second- and third-row elements than the first-row ones.[24] The bond angles around the Ge center of **1** and **2** have been predicted to be about 90°, i.e., Ge uses mainly its three valence p-orbitals for bonding in these species. Thus, the inversion process is expected to be much less favored, as compared to the internal rotation. It should be pointed out that **TS1/2** is predicted here, unexpectedly, to be lower than **2** energetically by 0.2 kcal mol^{-1} at the G2+ level of theory, even though **TS1/2** has been shown by IRC calculations to connect species **1** and **2**. This may probably result from the fact that **TS1/2** as optimized above at the MP2(FU)/6-31+G(d,p) level does not correspond exactly to the maximum along the reaction path with respect to G2+ energies.[25] However, data in Figures

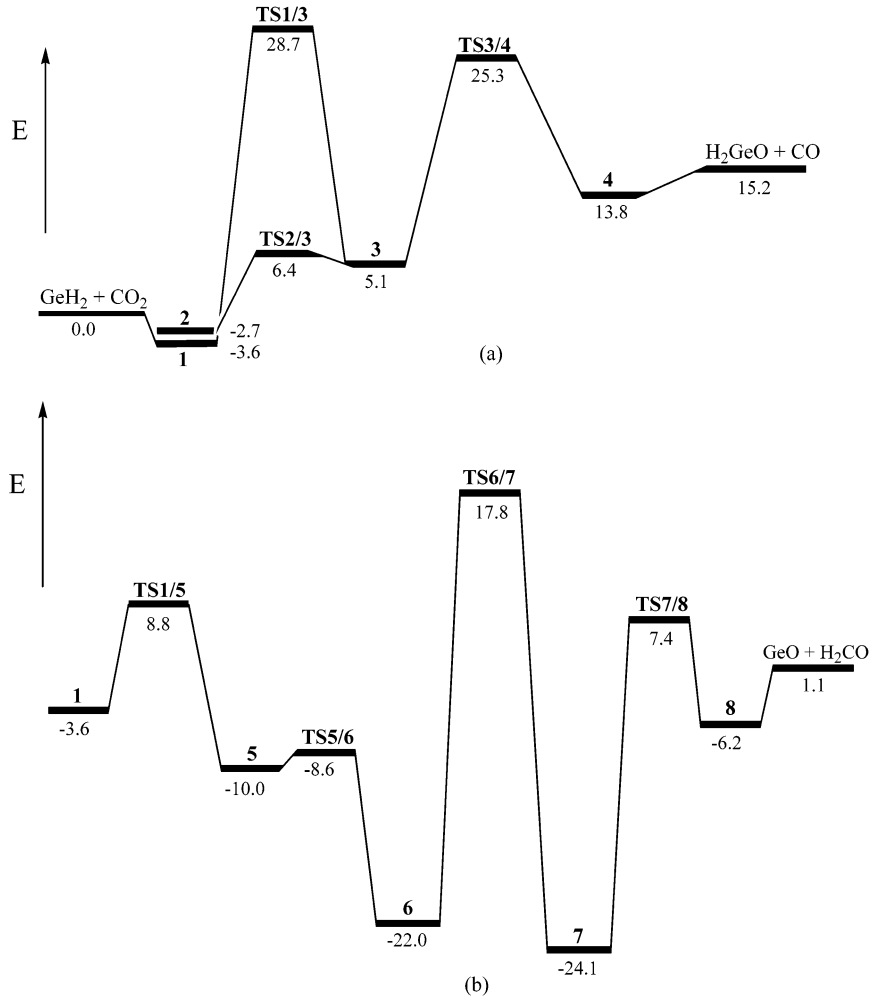

Figure 3. Schematic G2+ potential energy profiles (not drawn to scale) of the reactions studied: (a) pathway 1b and (b) pathway 2. Relative energies are in kcal mol^{-1}.

1 and 2 reveal that **TS1/2** is a late TS structure with most of its geometrical parameters closer to those of **2** than of **1**. In addition, the value of 0.2 kcal mol^{-1} is much smaller than the absolute average deviation of 1.21 kcal mol^{-1} of the G2 method from experiment[26] and thus should not be overemphasized. Hence, it is not unreasonable to take the activation energy for the conversion of **1** to **2** by internal rotation via **TS1/2** to be very near the energy difference between the two isomers, namely 0.9 kcal mol^{-1}.

3.2. Reaction 2: 1 → GeO + H_2CO. The decomposition of **1** to GeO and H_2CO is accomplished by four consecutive rearrangements followed by a bond dissociation (reaction pathway 2). Intermediates **5**, **6**, **7**, and **8** are formed via TS structures **TS1/5**, **TS5/6**, **TS6/7**, and **TS7/8**, with barriers of 12.4, 1.4, 39.8, and 31.5 kcal mol^{-1}, respectively. Finally, **8** decomposes to GeO and H_2CO without a barrier but an endothermicity of 7.3 kcal mol^{-1} (Figure 3). It is thus seen that the rearrangement of **6** to **7** has the largest activation energy and hence this is the rate-determining step of reaction 2 in terms of activation energy only. It should be pointed out that a TS structure for the rearrangement of **2** to **5** has been searched for but could not be found.

It is interesting to note from Table 2 that energies relative to that of reactants $GeH_2 + CO_2$ are negative for the molecular complexes **1**, **2**, and **8**, but positive for **4**. The Mulliken atomic charges for the atoms of the free/complexed subunits involved in the complexation are the following: Ge = 0.11/0.11 for GeH_2 and O = −0.33/−0.36 for CO_2 of **1** and **2**, Ge = 0.47/0.57 for H_2GeO and C = 0.14/0.21 for CO of **4**, and Ge = 0.47/0.50 for GeO and O = −0.33/−0.30 for H_2CO of **8**. Thus, the complexing atoms of the two subunits of **1**, **2**, and **8** have opposite charges, while in the case of **4**, they carry charges of the same sign. In addition, the ionic attraction along the Ge••••O bond is expected to be larger in **8** than in **1** and **2**. This perhaps accounts for the above predicted relative energies. As for the other stable isomeric structures **3**, **5**, **6**, and **7**, only **3** is less stable than ($GeH_2 + CO_2$). This is perhaps caused by the strain involved in the three-membered ring of **3**.

3.3. Comparison with $SiH_2 + CO_2$. The silicon analogues of the two reaction pathways 1b and 2 have been studied by Becerra et al.[8] The G2 potential energy surfaces of $SiH_2 + CO_2$ reported by them are in good qualitative accord with the G2+ PES of $GeH_2 + CO_2$ depicted in Figure 3. The only obvious difference between these two sets of results is in pathway 1b of the two reactions. For $SiH_2 + CO_2$, the intermediates involved in this pathway, Si analogues of **3** and **4**, are more stable than the reactants, while this is certainly not true for $GeH_2 + CO_2$. These differences in relative energies may be related to the energies of the two reactions under comparison: the reaction $SiH_2 + CO_2 \rightarrow H_2SiO + CO$ is exothermic by 17.7 kcal mol^{-1}, while the reaction $GeH_2 + CO_2 \rightarrow H_2GeO + CO$ is endothermic by 15.2 kcal mol^{-1}.

Regarding pathway 2 of the reactions producing SiO/GeO + H_2CO, the energy profiles are quite similar. Both involve very stable intermediates **6** and **7**. Also, for the reactions to proceed, both of these intermediates have to climb out of very

deep potential wells. The rate-determining step of the Ge reaction has a barrier of about 40 kcal mol^{-1}, while the Si reaction has two elementary steps with barriers of about 33 kcal mol^{-1}.

In the work reported by Becerra et al.[8] experimental gas-phase kinetics studies were also carried out for the reaction between SiH_2 and CO_2. It was found that the formation of $H_2SiO + CO$, via a mechanism analogous to our pathway 1b, is consistent with the kinetics data and supported by the G2 calculations. In addition, direct abstraction of an oxygen atom from CO_2, as well as other potential pathways, can be ruled out. Furthermore, the mechanism deduced resembles that of $CH_2(^1A_1) + CO_2$.

In view of these results, and the striking similarities between the Si and Ge reactions, we may therefore conclude that the reaction between GeH_2 and CO_2 will lead to the formation of $H_2GeO + CO$. Also, the pathway involved should be **1/2** → **3** → **4** → $H_2GeO + CO$, instead of the direct dissociative pathway of **1/2** → $H_2GeO + CO$.

4. Conclusion

We have applied the high-level ab initio G2+ method to investigate the energy profiles of the reaction between GeH_2 and CO_2. The computational results indicate that the reactants first form isomeric species **1** and **2**, which may be regarded as loosely bound $H_2Ge\cdots OCO$ complexes. These complexes can then proceed to undergo dissociation reaction to eventually yield products $H_2GeO + CO$ or $GeO + H_2CO$. The G2+ results suggest that the former reaction is more likely to occur. Additionally, the dissociation of **1**/**2** should follow pathway 1b involving two intermediates, instead of proceeding along pathway 1a, which involves the direct cleavage of a CO bond. Also, a comparison between the present results and the theoretical as well as the experimental gas-phase kinetics data of the analogous reaction between SiH_2 and CO_2 is given.

Acknowledgment. The authors wish to thank their Department for financial allocation and their University for a Special Equipment Grant to support the acquisition of the workstations. They are also grateful to the Computer Services Centre of the Chinese University of Hong Kong for its allocation of computer time on its supercomputers. W.K.L. acknowledges the support of a grant from the Research Grants Council of the Hong Kong Special Administrative Region (Project No. CUHK4275/00P).

References and Notes

(1) Jasinski, J. M.; Becerra, R.; Walsh, R. *Chem. Rev.* **1995**, *95*, 1203.

(2) Gasper, P. P.; West, R. Silylenes. In *The Chemistry of Organic Silicon Compounds*; Rappoport, Z., Apeloig, Y., Eds.; Wiley: Chichester, UK, 1998; Vol. 2, Chapter 43, p 2463.

(3) Becerra, R.; Cannady, J. P.; Walsh, R. *J. Phys. Chem. A* **1999**, *103*, 4457.

(4) Becerra, R.; Cannady, J. P.; Walsh, R. *Phys. Chem. Chem. Phys.* **2001**, *3*, 2343 and references therein.

(5) Koch, M.; Temps, F.; Wagener, R.; Wagner, H. G. *Ber. Bunsen-Ges. Phys. Chem.* **1990**, *94*, 645.

(6) Kistiakowsky, G. B.; Sauer, K. *J. Am. Chem. Soc.* **1958**, *86*, 1066.

(7) Kovac, D.; Jackson, J. E. *J. Phys. Chem. A* **2001**, *105*, 7579.

(8) Becerra, R.; Cannady, J. P.; Walsh, R. *J. Phys. Chem. A* **2002**, *106*, 4922.

(9) Becerra, R.; Boganov, S. E.; Egorov, M. P.; Nefedov, O. M.; Walsh, R. *Chem. Phys. Lett.* **1996**, *260*, 433.

(10) So, S. P. *J. Phys. Chem. A* **2001**, *105*, 4988.

(11) Frisch, M. J.; Trucks, G. W.; Schlegel, H. B.; Scuseria, R. E.; Robb, M.A.; Cheeseman, I. R.; Zakrzewski, V. G.; Montgomery, J. A., Jr.; Stratmann, R. E.; Burant, J. C.; Dapprich, S.; Millam, J. M.; Daniels, A. D.; Kudin, K. N.; Strain, M. C.; Farkas, O.; Tomasi, J.; Barone, V.; Cossi, M.; Cammi, R.; Mennucci, B.; Pomelli, C.; Adamo, C.; Clifford, S.; Ochterski, J.; Petersson, G. A.; Ayala, P. Y.; Cui, Q.; Morokuma, K.; Malick, D. K.; Rabuck, A. D.; Raghavachari, K.; Foresman, J. B.; Cioslowski, J.; Ortiz, J. V.; Baboul, A. G.; Stefanov, B. B.; Liu, G.; Liashenko, A.; Piskorz, P.; Komaromi, I.; Gomperts, R.; Martin, R. L.; Fox, D. J.; Keith, T.; Al-Laham, M. A.; Peng, C. Y.; Nanayakkara, A.; Gonzalez, C.; Challacombe, M.; Gill, P. M. W.; Johnson, B.; Chen, W.; Wong, M. W.; Andres, J. L.; Gonzalez, C.; Head-Gordon, M.; Replogle, E. S.; Pople, J. A. *GAUSSIAN 98*, Revision A.7; Gaussian, Inc.: Pittsburgh, PA, 1998.

(12) Curtiss, L. A.; Raghavachari, K.; Trucks, G. W.; Pople, J. A. *J. Chem. Phys.* **1991**, *94*, 7221.

(13) Pople, J. A.; Head-Gordon, M.; Fox, D. J.; Raghavachari, K.; Curtiss, L. A. *J. Chem. Phys*. **1989**, *90*, 5622.

(14) Curtiss, L. A.; Jones, C.; Trucks, G. W.; Raghavachari, K.; Pople, J. A. *J. Chem. Phys*. **1990**, *93*, 2357.

(15) Gronert, S. *J. Am. Chem. Soc.* **1993**, *115*, 10258.

(16) Scott, A. P.; Radom, L. *J. Phys. Chem*. **1996**, *100*, 16502.

(17) Gonzalez, C.; Schlegel, H. B. *J. Chem. Phys.* **1989**, *90*, 2154.

(18) Gonzalez, C.; Schlegel, H. B. *J. Chem. Phys.* **1990**, *94*, 5523.

(19) Vilkov, L. V.; Tarasenko, N. A. *Zh. Struct. Khim.* **1969**, *10*, 1102.

(20) Gildewell, C.; Liles, D. C. *J. Chem. Soc., Chem. Commun.* **1979**, 93.

(21) Cetinkaya, B.; Gümrukcü, I.; Lappert, M. F.; Atwood, J. L.; Rogers, R. D.; Zaworotko, M. J. *J. Am. Chem. Soc.* **1970**, *102*, 2088.

(22) Smith, G. R.; Guillory, W. A. *J. Chem. Phys.* **1972**, *56*, 1423.

(23) Whitnall, R.; Andrews, L. *J. Phys. Chem.* **1990**, *94*, 2351 and references therein.

(24) Kutzelnigg, W. *Angew. Chem., Int. Ed. Engl.* **1984**, *23*, 272.

(25) Malick, D. K.; Petersson, G. A.; Montgomery, J. A., Jr. *J. Chem. Phys.* **1998**, *108*, 5704.

(26) Curtiss, L. A.; Carpenter, J. E.; Raghavachari, K.; Pople, J. A. *J. Chem. Phys*. **1992**, *96*, 9030.